

# Predicting subsurface soil layering and landslide risk with Artificial Neural Networks: a case study from Iran

FARZAD FARROKHZAD<sup>1</sup>, AMIN BARARI<sup>2\*</sup>, LARS B. IBSEN<sup>2</sup> and ASSKAR J. CHOBBASTI<sup>1</sup>

<sup>1</sup>Department of Civil Engineering, Babol University of Technology, Babol, Mazandaran, Iran

<sup>2</sup>Department of Civil Engineering, Aalborg University, Sohngårdsholmsvej 57, 9000 Aalborg, Denmark; \*ab@civil.aau.dk, \*amin78404@yahoo.com

(Manuscript received November 9, 2010; accepted in revised form March 17, 2011)

**Abstract:** This paper is concerned principally with the application of Artificial Neural Networks (ANN) in geotechnical engineering. In particular the application of ANN is discussed in more detail for subsurface soil layering and landslide analysis. Two ANN models are trained to predict subsurface soil layering and landslide risk using data collected from a study area in northern Iran. Given the three-dimensional coordinates of soil layers present in thirty boreholes as training data, our first ANN successfully predicted the depth and type of subsurface soil layers at new locations in the region. The agreement between the ANN outputs and actual data is over 90 % for all test cases. The second ANN was designed to recognize the probability of landslide occurrence at 200 sampling points which were not used in training. The neural network outputs are very close (over 92 %) to risk values calculated by the finite element method or by Bishop's method.

**Key words:** Modelling, subsurface soil layering, landslide, Artificial Neural Network.

## Introduction

### Context and literature review

In geotechnical engineering, it is not uncommon to encounter problems that are very complex and not well understood. In most cases, the mathematical models used to solve such problems attempt to make up for our lack of physical understanding by either simplifying the problem or incorporating several assumptions. Such models may also be designed to produce solutions with a specific structure, chosen in advance, which may be suboptimal for the case at hand. Consequently, many mathematical models fail to simulate the complex behaviour of geotechnical engineering problems (Rizzo & Dougherty 1994). Analyses based on the finite element method provide a better assessment of geotechnical engineering problems, but these are often costly and time-consuming.

These limitations of mathematical and finite element models make the problem of landslide prediction exceedingly difficult. Constitutive programs to determine the stability of slopes require many free parameters and a large amount of input data to calibrate. Therefore, practicing engineers prefer to employ simplified methods to assess subsurface layering and landslide risk. Such procedures are very useful in the preliminary design stages of a new project. If the landslide risk is high, then finite element analysis can be carried out to determine the stability of the slope with accuracy suitable to the subsequent design of structures. Artificial Neural Networks (ANNs) provide a very different approach to geotechnical prediction, with many advantages.

ANNs are model-independent, nonlinear systems capable of learning physical patterns from a set of input-output data pairs (Gardner & Dorling 1998). Since their results are based entirely on the data provided, ANNs neither simplify the physical nature of the problem nor incorporate any assump-

tions. At worst, the data provided to train the network are biased. However, ANNs can always be updated to obtain better results by presenting additional training examples as new data become available (Ghaboussi & Sidarta 1998).

Many authors have studied applications of ANNs to geotechnical engineering. A frequent theme is the prediction of load capacity based on pile driving data. Ellis et al. (1992) developed an ANN model for sands based on grain size distribution and stress history. Chan et al. (1995) developed a neural network as an alternative to pile driving formulae. Lee & Lee (1996) utilized neural networks to predict the ultimate bearing capacity of piles. Teh et al. (1997) used a neural network to estimate the static capacity of precast, reinforced concrete piles with a square section based on dynamic stress-wave data. Penumadu & Jean-Lou (1997) used neural networks to represent the behaviour of sand and clay soils.

It should be mentioned that over the last ten years, the authors have undertaken a comprehensive research program using ANN (Chobbasti et al. 2009; Farrokhzad et al. 2011a,b). It should also be noted that every ANN is highly specialized, and entirely dependent on the input data of the particular project. All aspects of training must be carefully controlled, and we perform many robustness tests to show that the predictions of the networks are independent of the dataset used.

### Research goals

We will now discuss the central aspects of our research in more detail, as a means of showcasing the broad applicability of ANNs to geotechnical engineering problems. To this end, a short introduction to subsurface soil layering is in order.

It is known that the engineering properties of soil vary from point to point due to the complex and imprecise physical processes associated with its formation. In contrast, civil engineering materials such as steel and concrete exhibit far

greater homogeneity and isotropy. In order to cope with the complexity of geotechnical behaviour and the spatial variability of soil, traditional engineering design models have been justifiably simplified (Jaksa 1995). Soil geology plays an important role in core material selection (for example, the construction of rock fill dams) and in geotechnical evaluations preceding the construction of major structures.

Layering is caused by a variety of pedological and geological processes, and has important consequences for the interpretation of soils and landscapes. Collecting adequate data on soil layering (soil classification, thickness of layers) can be difficult and expensive, sometimes requiring a series of experiments. Therefore, a method of predicting the structure of subsurface soil layers from existing data would lead to significant cost reductions in soil geology and improved operational planning.

Accordingly, our first goal in this paper is to develop an ANN capable of predicting the type and depth of subsurface soil layers from easily collected geological data. Specifically, we will use the three-dimensional positions of layers observed in previously collected boreholes to train an ANN, then test the network's capacity to predict soil layers under an arbitrary location on the surface. The training and testing data were collected from the Mazandaran province of northern Iran.

Our second goal is to train an ANN to correctly predict landslide risk in the region based on more elaborate geophysical data. We will compare the outputs of the network to landslide risk assessments made using the finite element method and Bishop's method.

The remainder of this paper is organized as follows. In Section 2, we point out some relevant theoretical aspects of landslides and ANNs. Section 3 describes in detail our method of designing and training an ANN for soil layer prediction and the performance of the network. Section 4 describes our ANN for landslide risk assessment, while it is followed by Section 5 as conclusions.

## Theory

### Landslides

"Landslides" are mass motions of soil resulting from partially drained shear failures of the surface and subsurface layers. Relatively small disturbances may trigger landslides, especially in areas where previous slides have reduced the residual shear strength of soil masses along their corresponding slip planes (Choobbasti et al. 2008).

The deformation of soil masses generally begins at or close to the toe of the slope, because this is where the shear strength of the soil is first exceeded. The deformation then progresses retrogressively along the shear zones. Movements of the unstable soil masses take place at points where a large local strain leads to structural failure. The characteristics of landslides depend on the geometry of the unstable soil mass, the pore pressure distribution (which in turn usually depends on the location of the phreatic surface), the pattern of deformation, and the speed of the movements.

Two common underlying factors are the mechanical properties of the soil skeleton and the fraction of saturation by

groundwater (Terzaghi & Peck 1967). Applying Terzaghi's concept of the effective stress in saturated soil, the stress-strain behaviours of drained soil and dry soil can be assumed to be identical. Terzaghi's approach is detailed below.

The total stress  $\sigma_{ij}$  can be separated into an effective stress tensor  $\sigma'_{ij}$  and the pore pressure  $u$  as follows:

$$\sigma_{ij} = \sigma'_{ij} + u \cdot \delta_{ij} \quad (i, j = 1, 2, 3) \quad (1)$$

where  $\delta_{ij}$  is the Kronecker delta. The deformation of the soil skeleton only depends on changes in the effective stresses  $\sigma'_{ij}$ .

Shear failures occur along the shear planes forming the boundaries between moving masses of water-saturated dense soils or rocks. These failures may be caused by the deformation of partially undrained masses (Bekele et al. 2010). The word "landslide" is employed by the authors to describe such failures. The term implies more than deformation of the masses; one or more blocks of practically solid soil or rock must actually move (Yesilnacar & Topal 2005). A shear failure is generally assumed to occur when the average shear stress along the sliding (or slip) surface is equal to the shear strength of the soil or rock. The shear strengths can be evaluated by field or laboratory tests (Terzaghi & Peck 1967).

Given that landslides are a consequence of uneven draining in saturated soils and rocks, they lead to progressive failure of the structure and erode the residual strength of the layers. Thus, existing landslides may continue to slip at an average shear stress considerably less than the drained peak strength of the soil or rock. The drained peak strength can be measured by conventional tests (such as triaxial or direct shear tests of the completely drained material — Yilmaz 2009a).

The first sign of an imminent landslide is the appearance of surface cracks in the upper part of the slope. These cracks are perpendicular to the direction of movement. They may gradually fill with water, reducing the effective normal stress in the soil along the shear planes. This process may further degrade the soil's resistance. The speed of a landslide during the primary failure is controlled mainly by the nature of the materials involved and the overall shape (including steepness) of the failure surface.

With respect to the materials involved, it is known that soil with more loosely packed particles has a larger difference between the drained and undrained strengths. This is true for both sands and clays. When saturated, these materials are also known as "quicksand" and "quick clay"; even a small disturbance can cause their structures to collapse. Both types of soils are characterized by liquefaction failure (Lee et al. 2004).

In this paper, both subsurface layering and landslide analysis are assessed using artificial neural networks. Before continuing, we will therefore briefly introduce this form of modelling.

### Artificial Neural Networks

Neural networks are intuitively appealing structures based on a crude, low-level model of biological neural systems. Even a simple network is capable of modelling extremely complex nonlinear functions. They also excel at bypassing the "dimensionality problem" that bedevils other forms of

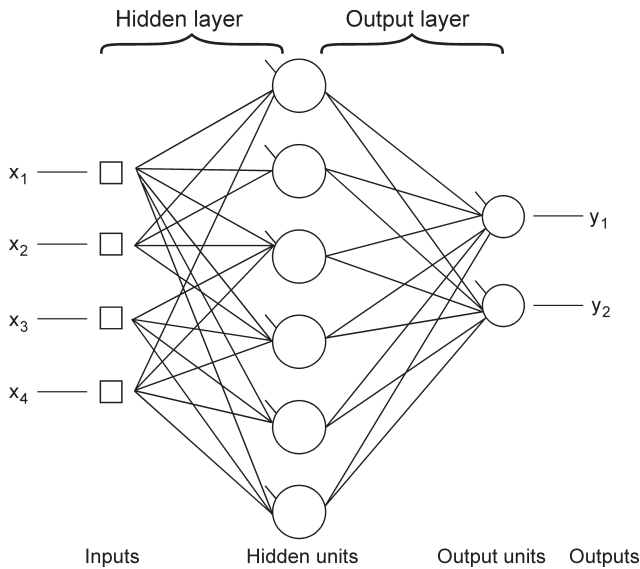


Fig. 1. Structure of Artificial Neural Network.

non-linear modelling, which often require a very large number of variables.

Neural networks learn by example. The researcher gathers representative data, then invokes a training algorithm to find a network structure that reproduces the data. A typical feed-forward network is shown in Fig. 1. The nodes are arranged in layers, with any given node transmitting its information to all nodes in the layer below. The input layer serves only to introduce the values of the input variables. The output layer is used to classify the data.

When the network is presented with data, the input variable values are placed in the input nodes. These values are used to generate signals in the first hidden layer, and then the hidden values are used to generate the output layer. The network calculates the signal for a hidden node or output node by performing a weighted sum of the outputs from units in the preceding layer and subtracting a threshold. This value is then passed through an activation function to produce the outputs of the node. The output layer signals are therefore a result of the entire network (Farrokhzad et al. 2011b).

**Predicting subsurface soil layering with ANNs**

**Data collection**

Babol (Fig. 2), a city in the Mazandaran province of northern Iran, is our study area for subsurface soil layering. The city is located approximately 20 kilometers south of the Caspian Sea, on the west bank of the Babolrood River. The region receives abundant annual rainfall. Babolrood has two types of river terraces, denoted H<sub>1</sub> and H<sub>2</sub>. H<sub>1</sub> terraces have a low level surface level, with heights of 1 to 2.5 m and widths of 0 to 150 m. In some sections of the river, these terraces mark the boundary of the active (yearly) flood plain. In other sections, they represent an alternative flood plain (diacritic of active-alternative flood plain from 20-year flood plain).



Fig. 2. Map of areas under study.

H<sub>1</sub> terraces consist of fine-grained and unconsolidated alluvial materials. H<sub>2</sub> terraces are referred to as river terraces. They have higher surface levels, 4 to 6 m, and support compact vegetation. They consist of Aeolian deposits (loess).

This research makes use of data from 40 borehole logs collected in the study area by a different institute of geotechnical engineering and seismology, for different research purposes. The boreholes cover a region of about 7.8 square kilometers, separated into five zones by imaginary lines (Fig. 3). Thirty of the logs, with depths of 10 m to 30 m, were used to train and test our ANN (Fig. 4).

The properties of the soil layers were determined by field examination and by laboratory index testing of benchmark soils following standard procedures. During the survey, we bored many shallow holes, examined and classified the samples, and created a soil map of the region. The samples were tested in the laboratory to determine their grain size distribution, plasticity, and compaction characteristics (Allen & Tadesse 2003). Table 1 shows the estimated properties of the soil types, including grain size distributions and Atterberg limits, engineering classifications, and the physical properties of the major layers.

**The soil layer ANN**

To train the Artificial Neural Network, we need a set of known input and output pairs (Basheer 1998). The available input-output pairs are usually divided into two sets. The learning or training set is used to determine the connection weights ( $w_{ij}^k$ )<sup>1</sup> (Agrawal et al. 1997) in the network. The testing set is used to measure the performance of the neural network after training. In this study, 70 % of the data were used for training and 30 % were used for testing. We tried other ratios, but this one yielded the best results.

$$y_i^k = f(y_i^k) = f\left(\sum_{j=1}^{n_{k-1}} w_{ij}^k y_j^{k-1}\right)$$

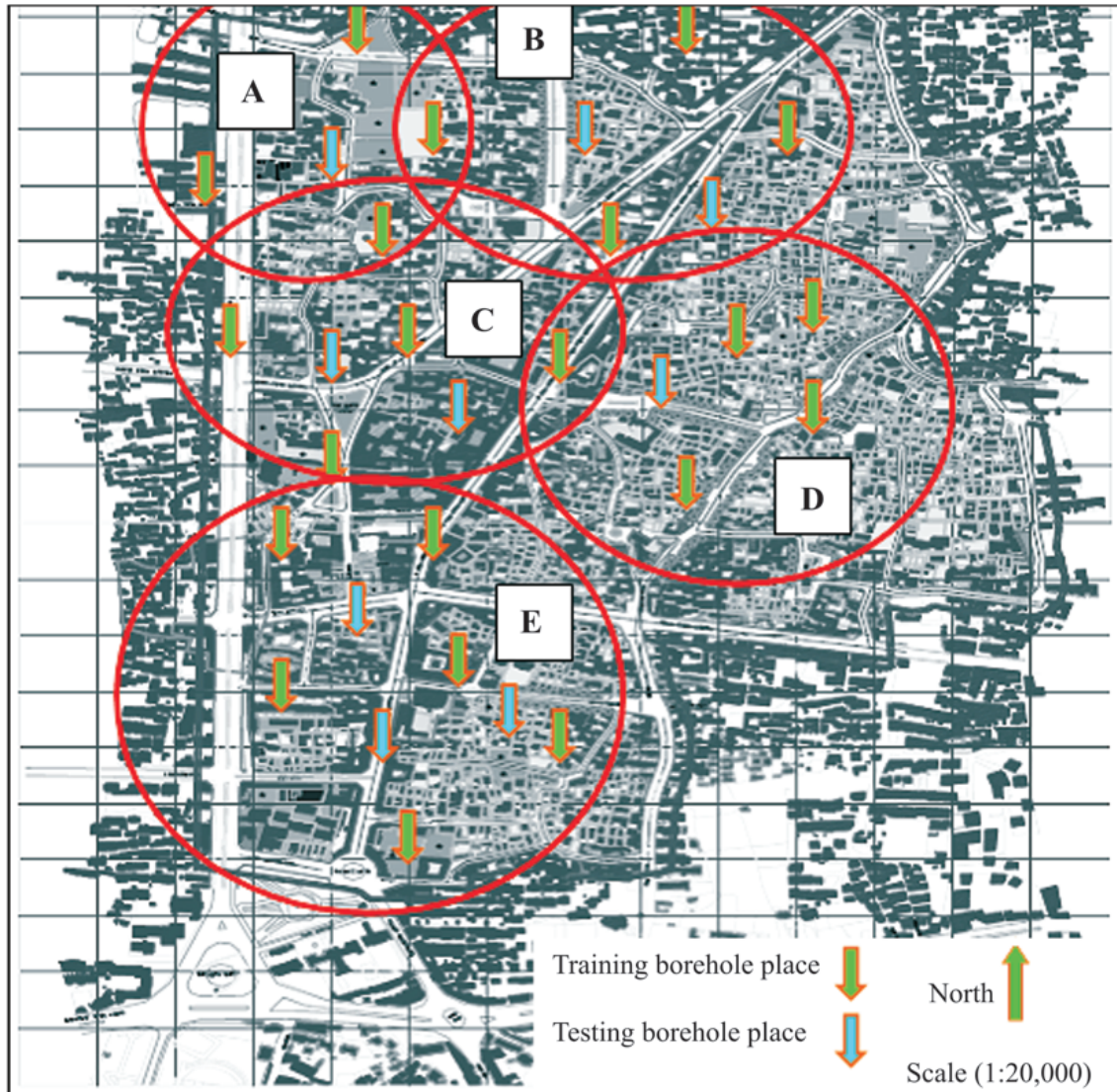


Fig. 3. Plan of some borehole places in 7.80 km<sup>2</sup> in western part of Babol.

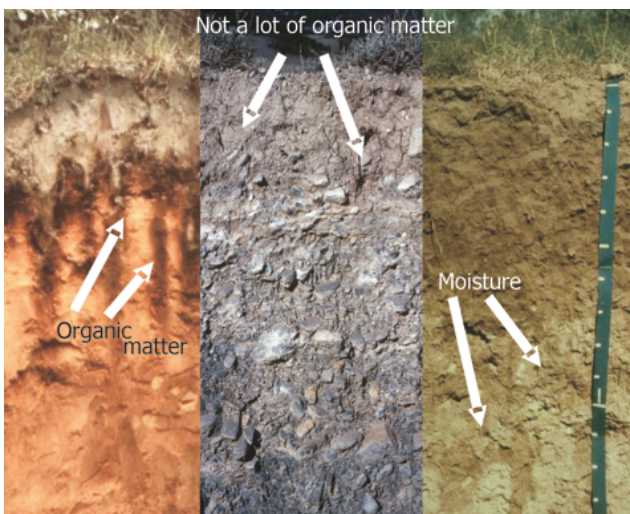


Fig. 4. Representative of soil profiles in study area.

A case study was conducted to evaluate the usefulness of the ANN approach and determine the optimal structure and algorithm. The inputs to the network were a set of soil formative environmental factors; the output was a set of similarity values mapped to soil classes. The classes are those defined by the Unified Soil Classification System (USCS) based on the particle size distribution and other properties that affect their usefulness as construction materials.

We tested this network's performance under five supervised learning (training) algorithms: back-propagation, conjugate gradient descent, Levenberg-Marquardt, quick propagation, and delta-bar-delta. Each training method yielded different results. In this case, performance is defined as the root-mean-squared (RMS) error of the output patterns produced by the network on the testing dataset.

The RMS values shown in Table 2 are based on a back-propagation neural network with one hidden layer. Back-propagation is the best known training algorithm for neural networks, and is still one of the most useful. It has a lower

**Table 1:** Samples of data collected from western part of Babol.

Field description of soils	Depth (m)	Sample	SPT blows count (N)	% Passing Sieve No. 200	Moisture content w. %	Liquid limit LL	Plastic limit PL	Soil classification	Unconfined compression qu (kg/cm <sup>2</sup> )	Internal friction angle φ°	Cohesion c (kg/cm <sup>2</sup> )
Medium stiff lean clay	0										
	1	SPT1	2/15, 2/15, 3/18 (5/33 cm)	78.4	27.0	32.8	21.9	CL			
	2	V1 D1		92.4	29.7			CL			0.96
Medium stiff lean clay	3	SPT2	3/15, 3/15, 4/18 (7/33 cm)	93.4	26.2	42.1	21.2	CL	0.78		
Silty fine sand	4	V2		95.0	37.8			CL			
Medium stiff lean clay	4	D2		97.5	33.3			CH			0.74
Stiff fat clay	5	SPT3	3/18, 4/15, 5/15 (9/30 cm)	98.9	27.5	58.6	23.3	CH	1.70		
	5	V3						CH			1.38
	6	D3		95.7	28.1			CH			
Medium stiff lean clay	7	SPT4	2/15, 4/15, 7/15 (11/30 cm)	95.4	27.2	46.8	21.2	CL	1.0		
	8	V4		90	35.1			CL			0.53
Sandy silt and silty fine sand	9	SPT5	3/20, 4/15, 5/15 (9/30 cm)	54.7	23.9	28.1	NP	ML			
	10										
Silty fine sand along with layers of silty clay	11	SPT6	4/15, 4/15, 4/15 (8/30 cm)	42.9	21.4	26	15.3	SC			
	12	D4		39	26.1			SM			
	13	SPT7	3/15, 8/15, 8/15 (16/30 cm)	40.9	22.8	26.1	NP	SM			
Stiff fat clay	14	SPT8	5/16, 9/15, 11/15 (20/30 cm)	97.5	29.1			CH			
	14			98.4	28.4			CH	1.56		
	15	D5		95.2	28.1			CH			
Stiff dark fat clay	16	SPT9	3/15, 6/16, 8/13 (14/29 cm)	99.4	29.2	59.2	24.3	CH	2.4		
	17	D6		91.4	31.5			CH			
Medium stiff lean clay	18	SPT10	2/16, 4/15, 5/17 (9/32 cm)	94.8	29.1			CL			
End of boring	18			78.1	26	30.9	21.2	CL			

memory requirement than most algorithms, and usually reaches an acceptable level of error very quickly. However, it can be very slow to converge to the error minimum.

We tested networks with 3, 5, 7, 8, 9, 10, 11, 12 neurons in the hidden layer. Table 3 shows the results of this comparison. The network with 8 hidden neurons produced the smallest RMS error in this case study. This network's architecture is shown in Fig. 5.

The training phase is divided into epochs. In each epoch, every input-output pair in the training set is fed through the network once and used to adjust the network weights and thresholds. After each epoch the state of the network and the performance of the network on the testing set are recorded, so that if over-learning occurs the best network discovered during training can be retrieved. The number of epochs required to optimize the network in this research varied between 100 and 500. It is good practice to "shuffle" the training set in each epoch, presenting the input-output pairs to the network in a random sequence. (If the sequence never changed, the network might perform better for pairs at the end of the epoch.)

In addition to the primary choices described above, back-propagation models can be tuned using two parameters. The learning rate controls the size of the weight changes made by the training algorithm. A larger learning rate may lead to faster convergence, provided that the error surface is not too noisy (Penumadu & Zhao 1999). In the present work, we select a learning rate of 0.5. The momentum parameter causes the back-propagation algorithm to "pick up speed" if consecutive training pairs push the weights in the same direction. This property helps the network reach a global optimum by preventing it from getting trapped in local minima of the parameter space.

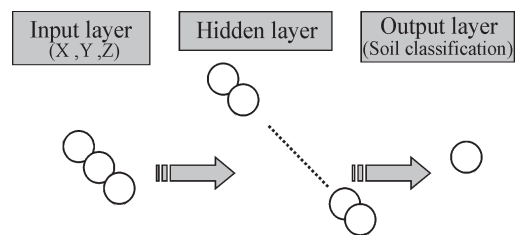


**Fig. 5.** Network architecture for prediction of subsurface soil layering in Babol.

**Table 2:** Results of research in order to Learning/training algorithm selection.

Supervised learning/training algorithms	Back propagation	Conjugate gradient descent	Levenberg-Marquardt	Quick propagation	Delta-Bar-Delta
RMS (%)	8	11	13.3	10.7	11.5

**Table 3:** Results of research in order to select the number of neurons in the hidden layer.

Number of neurons in the hidden layer	3	5	7	8	9	10	12
RMS (%)	14	11.7	10.9	7.5	9.8	12.1	13.3

**Results of the soil layer ANN**

Figure 6 presents the ANN’s predictions for the thickness of subsurface soil layers in three boreholes, and the actual layers obtained from digging the boreholes. As mentioned in the previous section, soils from the Babol study area were classified into four types: gravel, sand, silt and clay. In the case study, the input variables were simply the subsurface coordinates (x, y, z). For a given value of x and y, the network yields different soil types for different values of z (depth). The neural network results are very similar to the real data. In fact, the ANN model properly predicts the types of soil present in all three boreholes. The predicted thick-

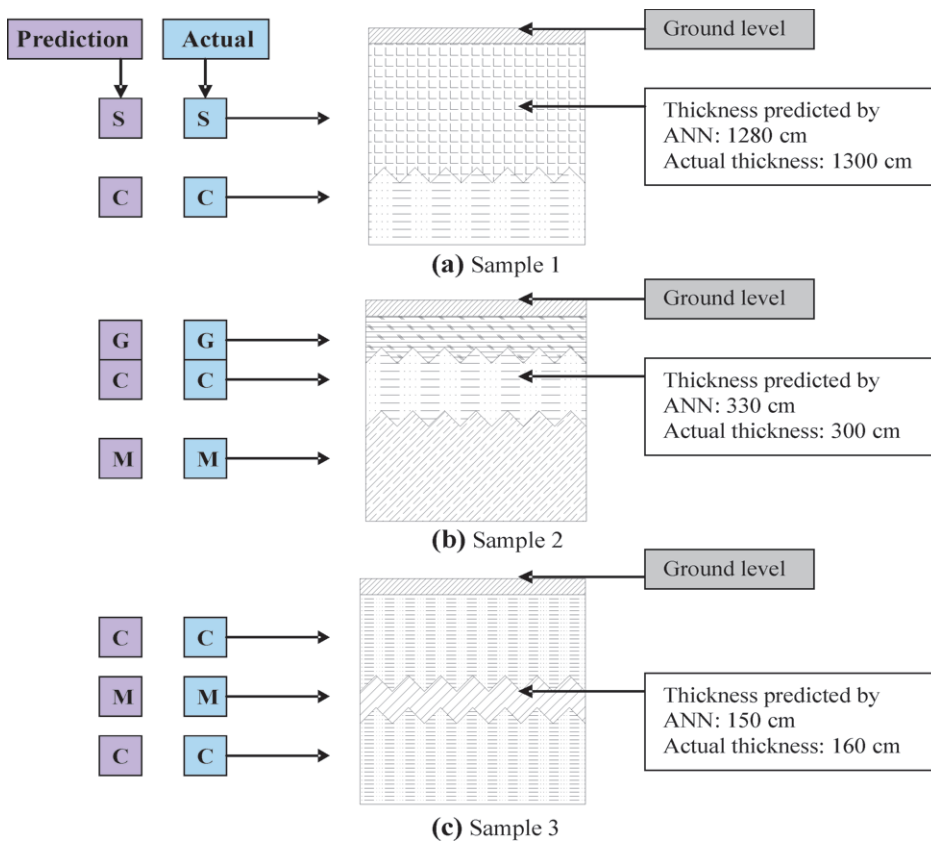
nesses of the three layers are 1280 cm, 330 cm and 150 cm. The corresponding actual thicknesses are 1300 cm, 300 cm and 160 cm.

Figure 7 plots the ratio of the predicted values to the actual values based on soil investigation for all samples in the testing set. If the predicted value and the true value are similar in all cases, then the points should all lie near the line  $y = 1$ . The average correlation of the ANN predictions with the true data in all cases is over 90 %. Thus, it can be concluded that the ANN method can accurately predict the depths of subsoil layers. This ANN is a viable prediction tool that can assist geotechnical engineers in making accurate and realistic predictions of the subsoil structure.

**An assessment of landslide risk in Shirgah**

Shirgah (Fig. 2) is located in the north of Iran, in Mazandaran province. The annual mean temperature of the terrain is 12.5 °C, and the annual mean precipitation is about 800 mm. The climate (from the Dommartan method) is humid. From a geological point of view, most of the units in this region are related to the Cenozoic Era. Marl, shale and silty stone are therefore prevalent, and the region is susceptible to landslides.

Before assessing risk on this slope, we dug several boreholes to obtain essential information such as details of the strata, moisture content, and the standing water level. Piezometer tubes were installed in the ground to measure changes in water level over time. These field investigations also included in situ and laboratory tests, photographs, a study of geological maps and memoirs to indicate probable soil conditions,



**Fig. 6. a, b, c** — Comparison between predicted results of ANN and soil profiles obtained from test boreholes.

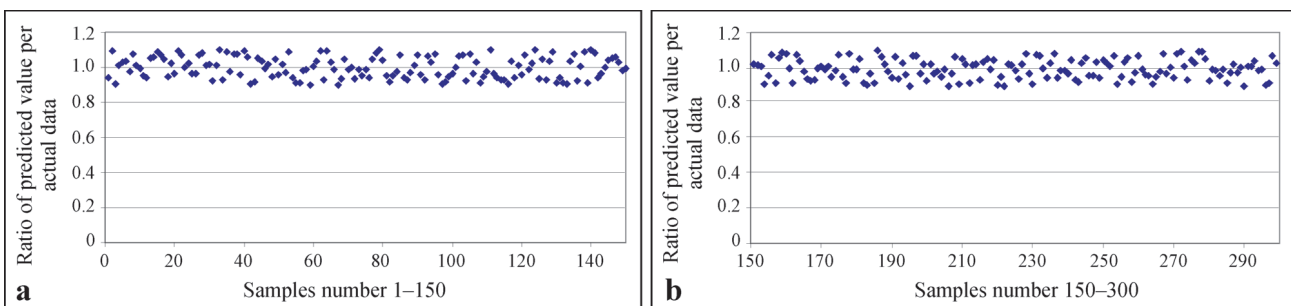


**Fig. 7.** Errors in the ANN for prediction of subsurface soil layers in test samples obtained from test boreholes.

visiting and observing the slope, examining records of previous instabilities, and plotting the topography (Fig. 8).

As with the case study described in Section 3, we tested several network structures, training parameters, and other criteria to find the ANN model that was most suitable for predicting landslide hazard in the region. After a number of trials, the best-performing ANN had four layers: an input layer of 8 neurons, an output layer of 2 neurons, and two hidden layers. All other aspects of the ANN model are identical to that used in Section 3.

In selecting the input variables (Fig. 9a,b) we hope to recognize the conditions which caused the slope to become unstable

and the processes which triggered that movement. If the network can achieve an accurate diagnosis, it will be possible to understand the landslide mechanisms and propose effective remedial measures. In the proposed model, the input parameters are the coefficient of cohesion ( $C$ ), the angle of the slope ( $\alpha$ ), the angle of internal friction ( $\phi$ ), distance from the slope edge ( $X$ ), the unit weight ( $\gamma$ ), the slope elevation ( $H$ ), the effective stress ( $\sigma'$ ), and the length of the slope ( $L$ ). The output variable is the slope stability.

In this research, we assume that the horizontal acceleration of an earthquake is constant. During an earthquake, the horizontal acceleration on the blocks may cause instability.

However, this acceleration also reduces the normal stresses on the contact plane and hence the friction to shear along the plane. The contribution of the cohesion coefficient to shear strength may be real (due to cementation) or apparent (due to asperities on the discontinuity plane). During an earthquake cementation may be broken, and asperities may be broken or overridden leading to non-fitting roughness patterns. In all cases cohesion and friction are permanently reduced. Hence, an earthquake not only adds unfavourable forces to a slope but may also permanently reduce the shear strength along discontinuity planes (Yilmaz 2009b).

The ANN models developed in this research were used to predict the slope stability for 7 sections (labeled  $\alpha, \beta \dots, \lambda$ ) in our study area (Fig. 8). Approximately 1000 input-output pairs, including inputs and outputs, were collected for the prediction of landslide risk. Among these data, 80 % were used for training and 20 % were used to validate the ANN.

The data cover a wide spectrum of soil Fish parameters. In order to test the performance of the ANN, 21 random cases were selected from the testing set for detailed predictions using the finite element method or Bishop's method (see Table 4).

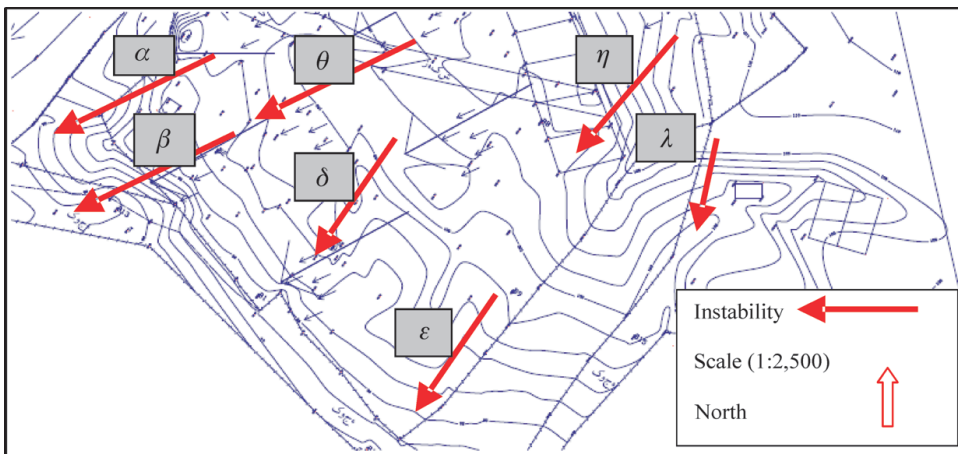


Fig. 8. Topography of study area and unstable zone.

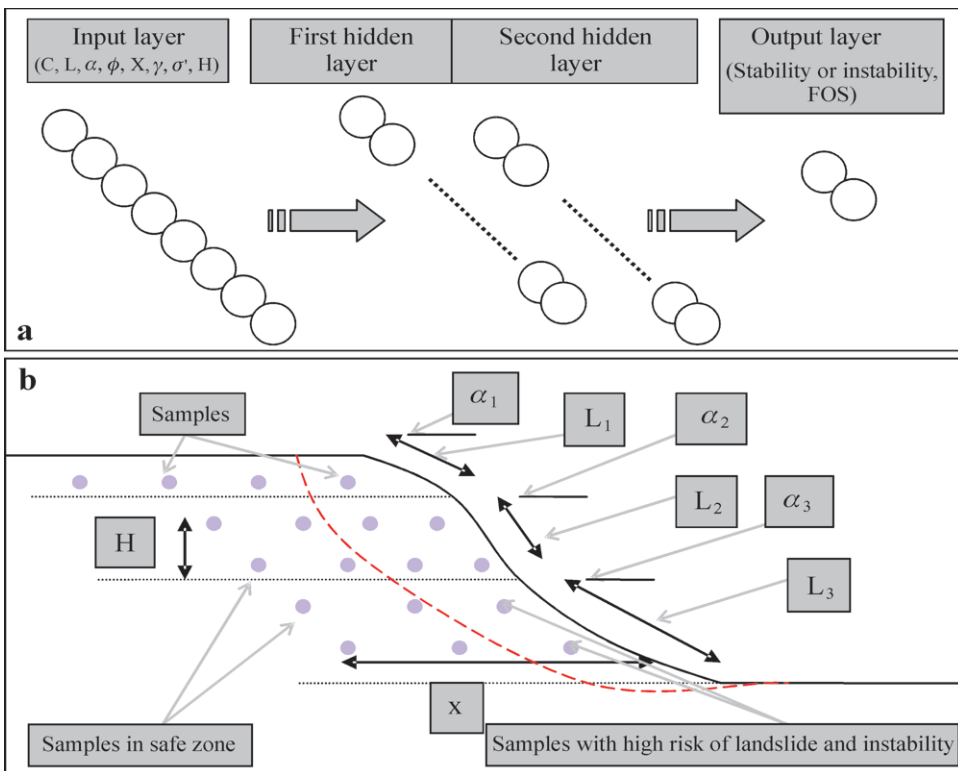
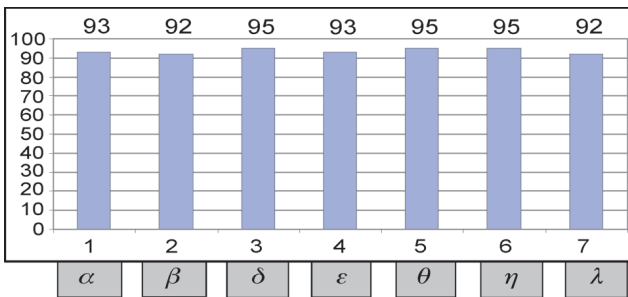


Fig. 9. a — Network architecture, b — Sample's coordinate and Stable and Unstable sample description.

**Table 4:** Selected case studies showing the actual modes of failure and prediction of the ANN.

Sample	C (kPa)	L (m)	$\alpha$ (°)	$\phi$	X (m)	$\gamma$ ( $\frac{\text{kN}}{\text{m}^3}$ )	$\sigma'$ ( $\frac{\text{kN}}{\text{m}^2}$ )	H (m)	Stability (Actual condition)	FOS (Actual condition)	Stability (Prediction of ANN)	FOS (Prediction of ANN)
$\alpha$ -1	13	45	35	19	2	21.2	15.96	12	instable	0.68	instable	0.72
$\alpha$ -2	13	45	35	19	5	21.2	39.91	12	instable	0.73	instable	0.79
$\alpha$ -3	13	45	35	19	10	21.2	79.82	12	instable	0.80	instable	0.82
$\beta$ -1	13	40	35	19	2	21.2	15.96	10	instable	0.77	instable	0.83
$\beta$ -2	13	40	35	19	5	21.2	39.91	10	instable	0.68	instable	0.69
$\beta$ -3	13	40	35	19	10	21.2	79.82	10	instable	0.71	instable	0.77
$\theta$ -1	10	63	18	22	2	20	6.62	15	instable	0.91	instable	0.86
$\theta$ -2	10	63	18	22	5	20	16.57	15	stable	1.03	instable	1.8
$\theta$ -3	10	63	18	22	10	20	33.14	15	stable	1.10	instable	1.09
$\varepsilon$ -1	13	72	22	19	2	21.2	9.21	9	instable	0.91	instable	0.97
$\varepsilon$ -2	13	72	22	19	5	21.2	23.02	9	stable	1.10	instable	1.02
$\varepsilon$ -3	13	72	22	19	10	21.2	46.05	9	stable	1.16	instable	1.05
$\delta$ -1	10	58	22	22	2	20	8.24	11	instable	0.87	instable	0.80
$\delta$ -2	10	58	22	22	5	20	20.60	11	instable	0.89	instable	0.92
$\delta$ -3	10	58	22	22	10	20	41.21	11	instable	1.04	instable	1.03
$\eta$ -1	10	40	36	22	2	20	14.82	5	instable	0.76	instable	0.85
$\eta$ -3	10	40	36	22	5	20	37.05	5	instable	0.81	instable	0.84
$\eta$ -3	10	40	36	22	10	20	74.10	5	instable	0.82	instable	0.84
$\lambda$ -1	13	35	38	19	2	21.2	17.81	12	instable	0.72	instable	0.68
$\lambda$ -2	13	35	38	19	5	21.2	44.53	12	instable	0.76	instable	0.71
$\lambda$ -3	13	35	38	19	10	21.2	89.06	12	instable	0.75	instable	0.76



**Fig. 10.** Accuracy of ANN in prediction of slope stability.

Figures 10 and 11 show the accuracy of the testing set (200 sampling points). In all cases the accuracy of the ANN model is over 92 %.

### Conclusion

In this investigation, we developed and trained two ANN models to demonstrate the suitability of the method for problems in geotechnical engineering. The first ANN predicts subsurface layering in the Babol region of Iran, and the second assesses landslide risk based on the physical characteris-

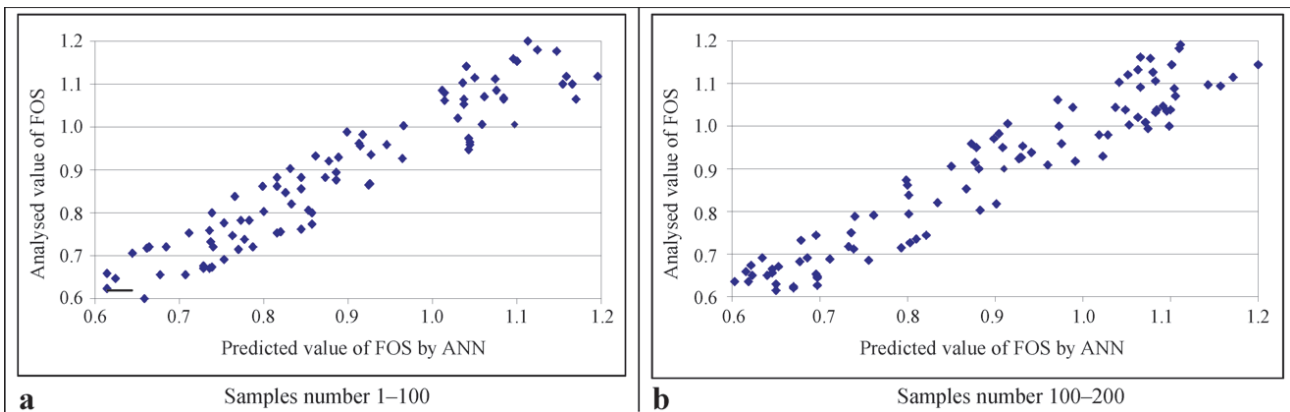


**Fig. 11.** Prediction of FOS versus true value.

tics of the slope and soil. Both neural networks provide very accurate results. The first network was tested on hand-collected borehole data, and the second network was compared to two classical mathematical models of landslide risk. The trained neural networks developed in this study are capable of predicting subsurface soil layering, the stability of slopes, and landslide risk in a specific study area with an acceptable level of confidence.

## References

- Allen A. & Tadesse G. 2003: Geological setting and tectonic subdivision of the Neoproterozoic orogenic belt of Tulu Dintu, western Ethiopia. *J. African Earth Sci.* 36, 1-2, 329-343.
- Agrawal G., Chameau J.A. & Bourdeau P.L. 1997: Assessing the liquefaction susceptibility at a site based on information from penetration testing. In: Kartam N., Flood I. & Garrett J.H. (Eds.): *Artificial neural networks for civil engineers: fundamentals and applications*. New York, 185-214.
- Basheer I.A. 1998: Neuromechanistic-based modeling and simulation of constitutive behavior of fine-grained soils. *Ph.D. Dissertation*, Kansas State University, Manhattan, KS.
- Bekele A., Dramis F., Fubelli G., Umer M. & Asrat A. 2010: Landslides in the Ethiopian highlands and the Rift margins. *J. African Earth Sci.* 56, 1, 131-138.
- Chan W.T., Chow Y.K. & Liu L.F. 1995: Neural network: An alternative to pile driving formulas. *J. Computers and Geotechnics* 17, 135-156.
- Choobbasti A.J., Barari A., Safaei M. & Farrokhzad F. 2008: Mitigation of Flourd landslide using non-woven Geosynthetic. *Bulgarian Geol. Soc. Rev.* 69, 1-3, 49-56.
- Choobbasti A.J., Farrokhzad F. & Barari A. 2009: Prediction of slope stability using artificial neural network — case study: Noabad, Mazandaran. *Arabian J. Geosci.* 4, 311-319.
- Ellis G.W., Yao C. & Zhao R. 1992: Neural network modeling of the mechanical behavior of sand. *Proc. Engineering Mechanics, ASCE*, 421-424.
- Farrokhzad F., Choobbasti A.J., Barari A. & Ibsen L.B. 2011a: Assessing landslide hazard using artificial neural network: case study of Mazandaran, Iran. *Carpathian J. Earth Environ. Sci.* 6, 251-261.
- Farrokhzad F., Choobbasti A.J. & Barari A. 2011b: Liquefaction microzonation of Babol city using artificial neural network. *J. King Saud Univ. (Sci.)*. Doi:10.1016/j.jksus.2010.09.003, in print.
- Gardner M.W. & Dorling S.R. 1998: Artificial neural networks (The multilayer perceptron) — A review of applications in the atmospheric sciences. *Atmospheric Environment* 32 (14/15), 2627-2636.
- Ghaboussi J. & Sidarta D.E. 1998: New nested adaptive neural networks (NANN) for constitutive modeling. *J. Computers and Geotechnics* 22, 1, 29-52.
- Gomez H. & Kavzoglu T. 2005: Assessment of shallow landslide susceptibility using artificial neural networks in Jabonosa River Basin, Venezuela. *Engineering Geol.* 78 (1-2), 11-27.
- Jaksa M.B. 1995: The influence of spatial variability on the geotechnical design properties of a stiff, overconsolidated clay. *Ph.D. Thesis, Univ. Adelaide, Adelaide*.
- Lee I.M. & Lee J.H. 1996: Prediction of pile bearing capacity using artificial neural networks. *Computers and Geotechnics* 18, 3, 189-200.
- Lee S., Ryu J.H., Won J.S. & Park H.J. 2004: Determination and application of the weights for landslide susceptibility mapping using an artificial neural network. *Engineering Geology* 71, 289-302.
- Penumadu D. & Jean-Lou C. 1997: Geomaterial modeling using artificial neural networks. *Artificial Neural Networks for Civil Engineers: Fundamentals and Applications, ASCE*, 160-184.
- Penumadu D. & Zhao R. 1999: Triaxial compression behavior of sand and gravel using artificial neural networks (ANN). *J. Computers and Geotechnics* 24, 207-230.
- Rizzo D.M. & Dougherty D.E. 1994: Application of artificial neural networks for site characterization using hard and soft information. Peters A. et al. (Eds.): *Proceedings of the 10th International Conference on Computational Methods in Water Resources. Kluwer Academic, Dordrecht* 12, 793-799.
- Teh C.I., Wong K.S., Goh A.T.C. & Jaritngam S. 1997: Prediction of pile capacity using neural networks. *J. Computing in Civil Engineering, ASCE*, 11, 2, 129-138.
- Terzaghi K. & Peck R.B. 1967: *Soil mechanics in engineering practice. John Wiley & Son, Inc., New.*
- Yesilnacar E. & Topal T. 2005: Landslide susceptibility mapping: a comparison of logistic regression and neural networks method in a medium scale study, Hendek region (Turkey). *Engineering Geology* 79, 251-266.
- Yilmaz I. 2009: A case study from Koyulhisar (Sivas-Turkey) for landslide susceptibility mapping by artificial neural networks. *Bull. Engineering Geol. Environment* 68, 3, 297-306.
- Yilmaz I. 2009: Landslide susceptibility using frequency ratio, logistic regression, artificial neural networks and their comparison: a case study from Kat landslides (Tokat-Turkey). *Computers and Geosciences* 35, 6, 1125-1138.